Development 133, 2925-2935 (2006) doi:10.1242/dev.02450

Segregation of telencephalic and eye-field identities inside the zebrafish forebrain territory is controlled by Rx3

Christian Stigloher[1], Jovica Ninkovic[1,*], Mary Laplante[2], Andrea Geling[1,†], Birgit Tannhäuser[1], Stefanie Topp[1], Hiroshi Kikuta[2], Thomas S. Becker[2], Corinne Houart[3] and Laure Bally-Cuif[1,‡]

Anteroposterior patterning of the vertebrate forebrain during gastrulation involves graded Wnt signaling, which segregates anterior fields (telencephalon and eye) from the diencephalon. How the telencephalic and retinal primordia are subsequently subdivided remains largely unknown. We demonstrate that at late gastrulation the Paired-like homeodomain transcription factor Rx3 biases cell specification choices towards the retinal fate within a population of bipotential precursors of the anterior forebrain: direct cell tracing demonstrates that retinal precursors acquire a telencephalic fate in embryos homozygous for the *rx3*-null allele *ckh*^{ne2611}, characterized by an enlarged telencephalon and a lack of eyes. Chimera analyses further indicate that this function of Rx3 is cell autonomous. Transfating of the eye field in the absence of Rx3 function correlates with a substantial posterior expansion of expression of the Wnt antagonist Tlc and the winged-helix transcription factor Foxg1. These results suggest that the process segregating the telencephalic and eye fields is isolated from diencephalic patterning, and is mediated by Rx3.

KEY WORDS: Zebrafish, Telencephalon, Eye field, Forebrain, Rx3

INTRODUCTION

The vertebrate forebrain is prefigured at embryonic stages by the anteriorly located telencephalon and retinae, the ventral hypothalamus and the caudal diencephalon. How their domains are initially established is incompletely understood.

Following the specification of forebrain identity during gastrulation, local organizers refine and maintain forebrain patterning (Foley and Stern, 2001; Wilson and Houart, 2004). One organizer, located at the anterior margin of the neural plate (ANB or ANR), controls development of anterior forebrain identities (Houart et al., 2002; Houart et al., 1998; Shimamura and Rubenstein, 1997). The ANB expresses the secreted factors Fgf3 and Fgf8 (Eagleson and Dempewolf, 2002), as well as potent Wnt antagonists (Houart et al., 2002). In zebrafish, one of these antagonists is the secreted Frizzled Related Protein (sFRP) Tlc. Ectopic expression of Tlc mimics ectopic ANB activity in telencephalic induction, and abrogation of Tlc function impairs the formation of telencephalon and eyes (Houart et al., 2002). Conversely, increased canonical Wnt activity, for instance by overexpression of Wnt8b normally produced in the posterior diencephalon (Kelly et al., 1995), or by the loss of function of Axin1, leads to an enlargement of the diencephalon at the expense of the telencephalon and eyes (Heisenberg et al., 2001; Houart et al., 2002; van de Water et al., 2001), and the lack of telencephalon can be corrected by increased levels of Tlc. Similarly, abrogation of the Wnt inhibitors Tcf3 or Six3 abolishes anterior forebrain development at the benefit of more posterior identities in zebrafish and mouse (Dorsky et al., 2003; Kim et al., 2000; Lagutin et al., 2003). These results suggest a model where the level of canonical Wnt activity, determined by the antagonism between a posterior local source and anterior local inhibitors, patterns forebrain development during gastrulation (Wilson and Houart, 2004).

Manipulations of Wnt or its antagonists at an early stage affect simultaneously the presumptive telencephalon and eye field, suggesting that these two domains are initially defined as one in their early response to Wnt activity. The factors controlling the later separation of the telencephalon and the eye field within the anterior forebrain are unknown. One candidate might be olSfrp1, a sFRP expressed in the anteriormost region of the neural plate in Medaka: abrogation of olSfrp1 function using morpholino antisense oligonucleotides produces embryos with reduced eyes and a complementarily enlarged telencephalon, without modifying diencephalic size (Esteve et al., 2004). How olSfrp1 acts at the cellular and molecular levels, and whether it indeed controls cell specification choices, however, remains unknown.

The specification of the eye field is correlated with sustained expression of Pax6, Six3 and Rx1-Rx3, shown to be crucial for eye development (Bailey et al., 2004; Graw, 2003; Hanson, 2003; Mathers and Jamrich, 2000). *Rx* genes encode paired-like homeodomain proteins. At late gastrulation, expression of the mouse *Rx* gene is intense in the eye field and is non-overlapping with the adjacent telencephalic field (Bailey et al., 2004; Chuang et al., 1999). A similar pattern is observed for zebrafish *rx3*, the earliest and only *rx* gene expressed at the open neural plate stage (Chuang et al., 1999). Knock-out of the single mouse *Rx* gene, and inhibition of *Xenopus* Xrx1 function, abolishes the formation of eye structures (Casarosa et al., 2003; Mathers et al., 1997). Conversely, ectopic expression of *rx1* and *rx2* by mRNA injection in zebrafish triggers an expansion of retinal tissue (Chuang and Raymond, 2001). These observations suggest that the *Rx* genes are involved in the specification or maintenance of retinal progenitors (Bailey et al., 2004), in contrast with the proposed later function of zebrafish and Medaka *rx3* in retinal evagination; in null

[1]Zebrafish Neurogenetics Junior Research Group, Institute of Virology, Technical University-Munich, Trogerstrasse 4b, D-81675, Munich, Germany and GSF-National Research Center for Environment and Health, Department Zebrafish Neurogenetics, Institute of Developmental Genetics, Ingolstaedter Landstrasse 1, D-85764 Neuherberg, Germany. [2]Sars Centre for Marine Molecular Biology, University of Bergen, Thormoehlensgt.55, N-5008 Bergen, Norway. [3]MRC Centre for Developmental Neurobiology, New Hunt's House, King's College London, SE1 9RT London, UK.

*Present address: GSF-National Research Center for Environment and Health, Institute of Stem Cell Research, Ingolstaedter Landstrasse 1, D-85764 Neuherberg, Germany
†Present address: Mischterlich and Partners, Postfach 330609, 80066 Munich, Germany
‡Author for correspondence (e-mail: bally@gsf.de)

Accepted 22 May 2006

mutants for Rx3 [*chokh* (*ckh*) and *eyeless* (*el*), respectively], early anterior genes such as *six3* or *pax6* are expressed, but the optic vesicle fails to evaginate (Kennedy et al., 2004; Loosli et al., 2003; Loosli et al., 2001; Winkler et al., 2000). Because forebrain patterning defects had not been noted, Rx3 was proposed to be an unusual member of the Rx family controlling retinal morphogenesis.

We describe here a zebrafish mutant, *ne2611*, with an expanded telencephalon and a lack of eyes. We report that *ne2611* is a null allele of *rx3*, and that retinal precursors in *ne2611* ectopically express *tlc* at late gastrulation and acquire a telencephalic fate. We reanalyzed the published allele ckh^{s399} and demonstrate that *tlc* and telencephalic expansion are also apparent in this mutant. These results identify Rx3 as a key determinant controlling specification choices between eye field and telencephalon during anterior forebrain patterning.

MATERIALS AND METHODS

Fish strains

Embryos of AB wild-type or ENU-treated fish were raised and staged according to Kimmel et al. (Kimmel et al., 1995). *chokh* (chk^{s399}) (Loosli et al., 2003) mutants were obtained by pairwise mating of heterozygous adult carriers. chk^{ne2611} fish were recovered in a small scale screen focusing on CNS defects. The screen setup followed that of Haffter et al. (Haffter et al., 1996), except that an incross was conducted in the F1 generation. The specific locus rate was 1/670 against the *golden* locus and 442 genomes were screened to recover *ne2611*.

Molecular identification of *ne2611*

The *rx3* locus of chk^{ne2611} mutants was analyzed for putative mutations by direct sequencing of PCR products (Sequiserve) of each of the three exons comparing homozygous wild-type with homozygous mutant embryos. Primers were designed to bind intronic sequences flanking the exons to include putative splice site mutations. An exception was exon 1, where the forward primer was designed containing the ATG-start site.

rx3_exon1_forward, 5′-GCACGAGGTTCAATGAGGC-3′;

rx3_exon1_ reverse, 5′-AAGTTAGAAGTTAGGATAAAGTTGTCAA-3′;

rx3_exon2_forward, 5′-TGCACTTTCTCACATATTTCTCACTG-3′;

rx3_exon2_ reverse, 5′-TATTATTGCTGTATTAGTTTGAACAGAA-3′;

rx3_exon3_forward, 5′-ATAAGCTCCTCAACTACATCTTTAACTT-3′; and

rx3_exon3_ reverse, 5′-AGACCACTGATTTTGAAGATACAAA-3′.

The only significant alteration was found at nucleotide position 382 of the coding sequence. This T to C transition leads to the introduction of a new *Sat*I endonuclease restriction site.

RNA and BAC injections

chk/rx3 cDNA (IMAGp998G108961Q) was obtained from RZPD (Deutsches Ressourcenzentrum für Genomforschung GmbH, www.rzpd.de) and subsequently subcloned into the pCS2+ Vector. chk^{ne2611}*/rx3* was cloned by PCR from reverse-transcribed RNA from homozygous *ne2611* mutant embryos, followed by direct cloning using the TOPO cloning kit (Invitrogen) and subcloning into pCS2+:

rx3_cDNA_forward, 5′-AAATCGTTCAATGAGGCTTGTT-3′; and

rx3_cDNA_reverse, 5′-TCTCATCTACCACGTCTTCCCTATA-3′

chk/rx3 and chk^{ne2611}*/rx3* capped RNA was synthesized using the Ambion mMessage mMachine Kit, following the recommended procedure. Capped RNA was injected at the concentration of 50 or 100 ng/μl into the embryos at the one-cell stage.

The BAC CHORB736A01233Q containing the *rx3* locus was obtained from RZPD, amplified and purified with the Large-Construct Kit (QIAGEN) and injected at a concentration of 35 ng/μl into embryos at the one-cell stage.

Bioinformatic analysis

The JPRED algorithm (Cuff et al., 1998) was used to find a nearly related secondary structure that has been analyzed in detail (http://www.compbio.dundee.ac.uk/~www-jpred/). The input was the protein sequence of Rx3 (ENSDARP00000022866) from the Sanger Centre zebrafish assembly version 4 (Zv4) using the ENSEMBL server. The primary output of the algorithm (1FJL.pdb) was used for further sequence and structure analysis using the MAGE software package version 6.36 (http://kinemage.biochem.duke.edu/software/mage.php).

Cell transplantations between *ne2611* and wild type

Wild-type donor embryos were injected with biotin-dextran (Molecular Probes) at the one-cell stage. Thirty to 40 cells were transplanted isotopically and isochronically onto the animal pole of shield-stage wild-type or *ne2611* embryos. Recipient embryos were processed at 30 hpf for immunochemical detection of the biotin tracer.

CLGY469 transgenic donor embryos were injected with 1.5% lysine-fixable (fluoro-ruby) Tetramethylrhodamine Dextran (10,000 M_r, Molecular Probes) in water (Ambion) at the one-cell stage. Cell transplantations were as previously described (Ho and Kane, 1990), with recipient and donor embryos maintained in the dark at all stages. Transplantation of around 10 cells was conducted in a homotypic manner at the animal pole at dome stage. The appropriate localization of transplanted cells was checked under fluorescent light, and donor and recipient embryos were documented and subsequently fixed at around 30 hpf.

Uncaging experiments

A solution of DMNB-Caged Fluorescein dextran and biotin, lysine fixable (5 mg/ml; Molecular Probes), was injected into one-cell embryos, which were allowed to develop further in the dark. At the early tailbud stage, the dye was activated in a few cells using a UV-beam (DAPI-channel) focused with a pinhole. Irradiated embryos were imaged at the 24 hpf stage, using the FITC-channel on a Zeiss Axioplan2 Microscope with a Zeiss Axiocam Hrm Camera and the Axiovision Software Package (Zeiss), and subsequently fixed overnight in 4% paraformaldehyde at 4°C and processed for anti-fluorescein immunocytochemistry.

In situ hybridization and immunohistochemistry

Probe synthesis, in situ hybridization and immunohistochemistry were carried out according to standard protocols (Hammerschmidt et al., 1996). The anti-Phospho-Histone H3 antibody (Upstate Biotechnology) was used in a final dilution of 1/200. Purified rabbit anti-GFP antibody (ams biotechnology) was used in a 1/500 to 1/1000 dilution. They were revealed using FITC-conjugated goat anti-rabbit secondary antibody (Jackson ImmunoResearch Laboratories) or Cy3-conjugated goat anti-mouse secondary antibody (Jackson ImmunoResearch Laboratories) (1/200). Embryos were scored and photographed under a Zeiss SV 11 stereomicroscope or a Zeiss Axioplan photomicroscope.

Isolation and mapping of the *CLGY469* insertion

CLGY469 was recovered in a retrovirus-mediated large-scale enhancer detection screen for its expression in the retina. The 3′ sequence flanking the insertion was identified by linker-mediated PCR as described previously (Ellingsen et al., 2005). This sequence (TAAAAAAAAATTTGGGGT-CAATATTACAAG) maps to chromosome 10, 37.390 base pairs upstream of the *rx3* locus (Sanger Centre zv5 release).

RESULTS

Selective enlargement of the anteriormost forebrain domain in *ne2611* mutant embryos

In *ne2611* homozygous embryos at 36 hours post-fertilization (hpf), the constriction separating the telencephalon from the diencephalon lies far posterior compared with wild type (wt) and the diencephalic ventricle is wide open (Fig. 1A,B) (n>100, 100% of cases); of the eye, only a small lens is visible (Fig. 1A′,B′, arrowheads). By contrast, the size of the nasal placodes and epiphysis were not affected.

Telencephalic expansion in *ne2611* was confirmed at the 15-somites stage with molecular markers (*emx3* – previously *emx1*-, *emx2*, *pax6.1*) (Fig. 1C,D; data not shown), and occurs along the anteroposterior (AP) and mediolateral axes. To determine whether this phenotype reflected broader AP patterning defects, we compared the relative sizes of the different forebrain and midbrain

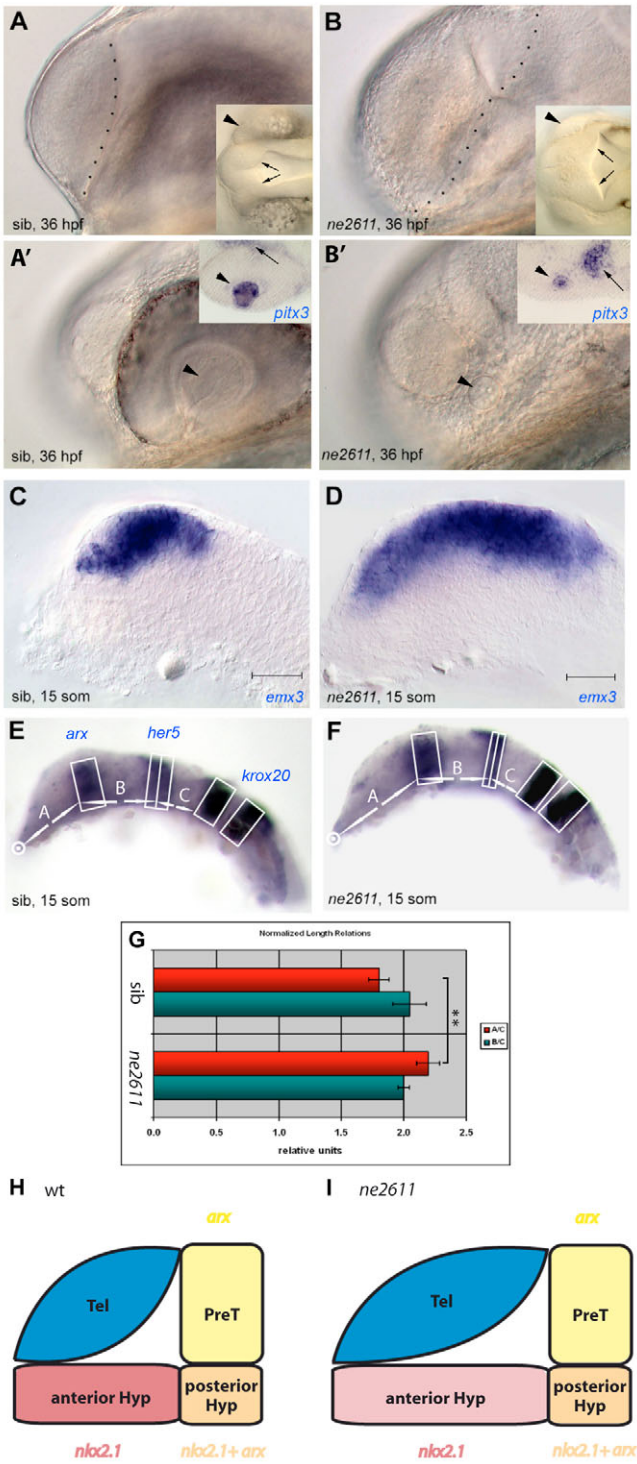

Fig. 1. Enlarged telencephalon and lack of retina in *ne2611*. All views are lateral, anterior left. (**A-B'**) Compared morphology of *ne2611* (B,B') and wild-type siblings (sib; A,A') at 36 hpf; views with parasagittal and lateral focus, respectively. (A,B) Note the enlarged telencephalon, delimited by a dashed line, in *ne2611*. Insets are dorsal views of the same embryos showing absence of the retina (arrowheads) and an expanded diencephalic ventricle (arrows) in *ne2611*. (A',B') Note the maintenance of a lens (arrowhead) in *ne2611*, albeit smaller than in wild-type siblings. Insets show expression of *pitx3*, molecularly identifying the lens (arrowheads) in both genotypes. The adjacent domain of *pitx3* expression (small arrows) is hypothalamic, it is displaced towards the lens in *ne2611* due to the absence of eyes. (**C,D**) Compared expression of the telencephalic marker *emx3* at the 15-somite stage in *ne2611* (D) and wild-type siblings (C); scale bar: 0.02 mm. The mutants display a massive anteroposterior enlargement of the *emx3* domain. (**E-G**) Relative anteroposterior sizes of the anteriormost forebrain (domain A) versus prethalamus, thalamus, pretectum and midbrain (domain B) at 15 somites in *ne2611* (E) compared with wild-type siblings (F). (G) Measurements are normalized to the size of the anterior hindbrain (domain C), and the domains are defined with the genes indicated in E. Bars indicate s.e.m. The difference in A/C length between wild type and *ne2611* is statistically significant (two-sample independent Student's *t*-test, *P* values are given in the text). (**H,I**) Schematic representation of the size of the different anterior forebrain territories in wild type versus *ne2611* siblings at 15 somites. The genes used as landmarks are color coded (yellow: *arx* only, prethalamus; red: *nkx2.1* only, anterior hypothalamus; orange: *arx*+*nkx2.1*, posterior hypothalamus). Prethalamus and posterior hypothalamus are unchanged in the mutants. The anterior hypothalamus appears elongated, but might be simply stretched (hence the lighter red color) by the anteroposterior enlargement of the telencephalon. Later, the anterior hypothalamus appears reduced or missing (see also Fig. S1I,J in the supplementary material).

domains (telencephalon, hypothalamus, prethalamus, thalamus, pretectum and midbrain). We used *lhx5* and *arx* as markers of the prethalamus and posterior hypothalamus at 15 somites, and *nkx2.1b* to reveal the anterior and posterior hypothalamus (Fig. 1E,F; data not shown; see also scheme in Fig. 1H,I). *her5* expression identified the midbrain-hindbrain boundary, and the size of the anterior hindbrain, limited by *krox20*, served as a reference to correct for variations in embryo length. We confirmed that *ne2611* embryos suffer from substantially elongated neural tissue anterior to the prethalamus (Fig. 1G, red bars, $P<0.01$, $n=10$ embryos measured for each genotype), and found that this phenotype is local, as the prethalamus itself, as well as structures located posterior to the *lhx5/arx* domain, is unchanged compared with wild-type siblings (Fig. 1G, blue bars, $P=0.75$, i.e. no significant change, $n=10$ embryos measured for each genotype) (size of the *arx* domain between wild type and *ne2611*: $P=0.15$, i.e. no significant change, $n=10$ embryos measured for each genotype) (schematized in Fig. 1H,I).

We next analyzed *ne2611* embryos for potential patterning phenotypes in telencephalic organization, as well as for the presence of cells having maintained molecular eye identity. We found that the telencephalon maintains a grossly normal dorsoventral polarity [see the dorsal and ventral telencephalic markers *emx3* (Fig. 3D-F) and *dlx2a* (see Fig. S1A,B in the supplementary material), respectively, and a normal mediolateral patterning (see Fig. S1C,D in the supplementary material)]. We noted, however, a perturbed expression of several regional markers, such as *flh* (telencephalic domain absent in *ne2611*) or *emx2* (scattered in *ne2611*) (see Fig. S1E-H in the supplementary material). This prompted us to analyze whether cells with retinal identity were present in the telencephalic domain of mutant embryos. We found that the enlarged telencephalon of *ne2611* never expressed retinal markers at post-somitogenesis stages (see *otx2* in Fig. 2A,B, and *atoh7* – previously *ath5* – and *vax2*, not shown).

The absence of expression of eye markers could result from the non-specification or the non-maintenance of eye precursors, and, to resolve this issue, we probed *ne2611* mutants for the expression of

the earliest eye-field markers. In order of appearance, we selected *rx3* (at 70% epiboly), followed by *rx1* and *rx2* (at the 3-somite stage) (Chuang et al., 1999; Chuang and Raymond, 2001). We found that *rx3* and *rx1* expression followed a normal spatiotemporal pattern in *ne2611* mutants compared with their wild-type siblings (Fig. 2C-H), but that their expression was lost during somitogenesis (not shown). By contrast, *rx2* was never expressed (Fig. 2I-K). Thus, an incomplete eye-field identity ($rx3^{+}$, $rx1^{+}$ but $rx2^{-}$) is specified in *ne2611*, but this transient phase is followed by the loss of expression of all retinal markers.

ne2611 is a null allele of *rx3/chokh*

Reduced or absent eyes characterize the zebrafish mutants *headless* (*hdl*; *tcf7l1a*) (Kim et al., 2000), *masterblind* (*mbl*; *axin1*) (Heisenberg et al., 2001; van de Water et al., 2001) and *chokh* (*ckh*; *rx3*) (Kennedy et al., 2004; Loosli et al., 2003; Rojas-Munoz et al., 2005). In addition, *hdl* and *mbl* embryos display various degrees of brain posteriorization leading to forebrain truncations, while the existing *ckh* alleles ckh^{s399}, ckh^{w29} and ckh^{hu499} were described as not affecting telencephalic development (Kennedy et al., 2004; Loosli et al., 2003). We found, however, that *ne2611* is allelic to *ckh* (23 embryos lacking eyes in 78 embryos from a *ne2611*/+×ckh^{s399}/+ intercross in two independent experiments). Sequencing of the *rx3* cDNA from *ne2611* embryos revealed a T to C transition within exon 2 in nucleotide position 382 (Fig. 3A), leading to a Serine to Proline substitution at amino acid position 128 of the Rx3 protein (T382N, Fig. 3B,C). Comparison using the JPRED algorithm with the structure of the *Drosophila* Paired homeodomain predicts this substitution to a coiled domain separating helix1 and 2 of the Rx3 homeodomain.

We were puzzled that no telencephalic defects had been reported in the studies of existing *ckh* alleles (Kennedy et al., 2004; Loosli et al., 2003; Rojas-Munoz et al., 2005). The above T382N mutation segregated with the *ne2611* telencephalon and eye phenotypes in DNA sequenced from eight independent embryos. The mutation creates a *Sat*1 restriction site that also segregated with loss of eyes and expanded telencephalon in more than 50 embryos tested by PCR and *Sat*1 digestion (not shown). In addition, we found that all eyeless embryos from a *ne2611*/+×ckh^{s399}/+ intercross, but no embryos with normal eyes from such crosses, had an enlarged telencephalon (not shown). We also could rescue both the retinal and telencephalic defects of *ne2611* embryos following injection of BAC CHORB736A01233Q, which contains the *rx3* locus (Sanger centre and RZPD; 79% of the mutant embryos were at least partially rescued, *n*=64; Fig. 3G-K). Finally, a re-analysis of ckh^{s399} revealed that mutant embryos display an enlarged telencephalon identical to *ne2611* (100% of cases, *n*=23; Fig. 3D-F, see also Fig. 4D). We conclude that *ne2611* is an allele of *ckh*, henceforth referred to as ckh^{ne2611}, and reveals a previously undiscovered role of Rx3 in telencephalic development.

As mentioned above, structural considerations predict that the $Rx3^{ne2611}$ protein is dysfunctional, and we found the telencephalic and eye phenotype caused by the *ne2611* mutation to be as severe as those of ckh^{s399}, which truncates the Rx3 homeodomain (Loosli et al., 2003). This suggests that *ne2611* might represent a null allele of *rx3*. To support this interpretation, we overexpressed $rx3^{ne2611}$ RNA in wild-type embryos. Ectopic expression of wild-type *rx3* mRNA produced embryos with head truncations at 24 hpf in a dose-dependent manner (10% of cases, *n*=56, Fig. 3L,N). By contrast, no morphological defects were noted following injection of $rx3^{ne2611}$ mRNA (Fig. 3M,N). These results suggest that *ne2611* is a null allele of *rx3*.

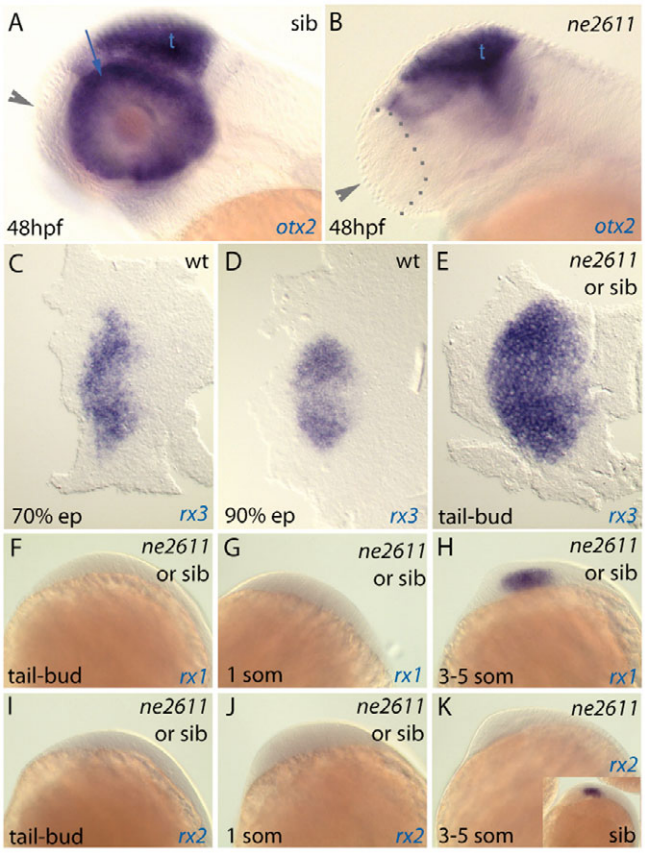

Fig. 2. The eye field is partially specified but is not maintained in *ne2611* mutants. All views, anterior left. (**A,B**) Expression of *otx2*, labeling the wild-type retina (A, blue arrow) but not the telencephalon, is absent in the enlarged telencephalon of *ne2611* sibling embryos (B). Lateral views; t, optic tectum; telencephalon (arrowhead) delimited by gray dots in B. (**C-H**) Expression of the earliest eye-field marker *rx3* (C-E; dorsal views of flat-mounted embryos), and of *rx1* (F-H; lateral views of whole embryos), is initiated normally in *ne2611*. (**I-K**) Expression of *rx2*, normally detected at 3-somites in wild type (K, inset), is never initiated in *ne2611* (K). Lateral views of whole embryos.

Rx3 controls patterning of the telencephalon and eye field at gastrulation

Zebrafish *rx3* expression is initiated at late gastrulation and is first restricted to the presumptive eye field and hypothalamus (Chuang et al., 1999), which abut the telencephalic primordium (Wilson and Houart, 2004). To determine whether the telencephalic phenotype of *ckh* reflects an early role of Rx3 in anterior neural plate development, we examined expression of telencephalic markers during these stages in both ckh^{ne2611} and ckh^{s399}.

tlc is one of the earliest markers of the presumptive anterior forebrain at late gastrulation, and is excluded from the hypothalamus and eye field (Houart et al., 2002) to become adjacent to the *rx3* domain at tail-bud stage (Fig. 4E,F). The earliest phenotype in both ckh^{ne2611} and ckh^{s399} mutants was the posterior expansion of *tlc* staining at the tail-bud stage (100% of ckh^{ne2611} mutant embryos, confirmed by genotyping, have expanded *tlc* expression, *n*>50; 24% of embryos from a cross between ckh^{s399} heterozygotes have a similar phenotype, *n*=82; Fig. 4A-D). Ectopic *tlc* expression was prominent from bud stage onwards (Fig. 4E-G). *emx3* and *foxg1* (*bf1*) also label the presumptive telencephalon, and we compared their expression with that of *tlc* expression in a time-course analysis. *foxg1* expression appeared identical in wild type and ckh^{ne2611}

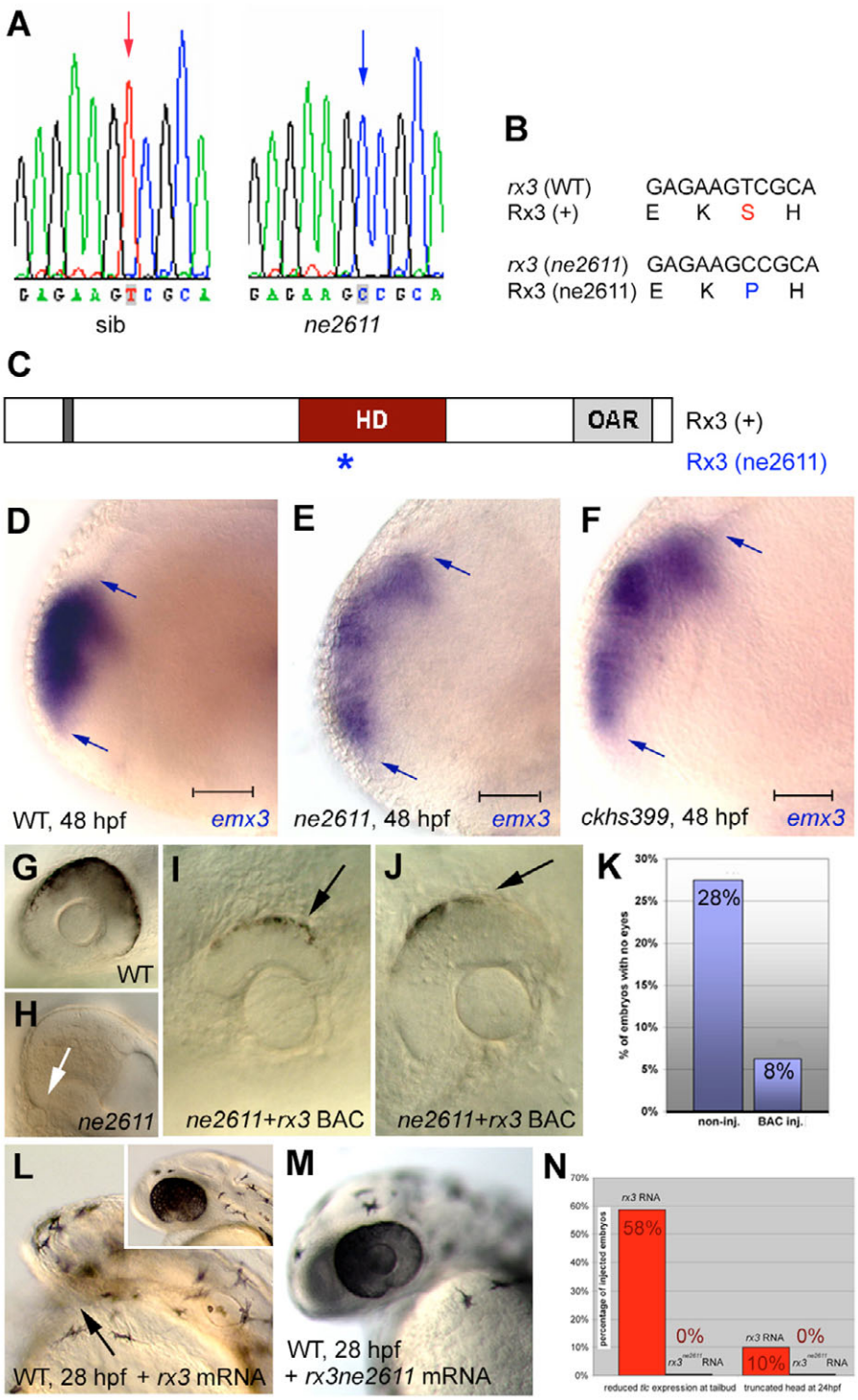

Fig. 3. *ne2611* is a new null allele of *rx3*. (**A**) Sequencing trace data of *rx3* cDNA from a *ne2611* mutant (right) and a wild-type sibling (left) reveals a T to C transition (arrows). (**B,C**) Rx3 protein sequences (B) and structures (C) in wild type (+) and *ne2611* mutants. The *ne2611* mutation leads to a Serine to Proline exchange within the Rx3 homeodomain (asterisk in C). Dark gray box, octapeptide; red box, homeodomain; light gray box, otp-aristaless-rx domain. (**D-F**) Expression of the telencephalic marker *emx3* in wild-type (D), *ne2611* (E) and *ckh*^{s399} (F) embryos at 48 hpf (lateral views, anterior left; scale bar: 0.02 mm). *ckh*^{s399} embryos display a telencephalic expansion similar to that of *ne2611* mutants. (**G-K**) Embryos from a *ne2611*/+×*ne2611*/+ cross were injected at the one-cell stage with BAC CHORB736A01233Q containing the *rx3* locus and are observed at 24 hpf. (I,J) Representative injected *ne2611* mutants; note the restoration of the retina compared with uninjected wild type (G) or *ne2611* (H; small lens in H indicated by the white arrow). (K) Percentage of embryos lacking eyes after BAC injection compared with non-injected embryos. BAC injection restored retinal development in 79% of mutant embryos. (**L**,**M**) Phenotypes triggered by ectopic expression of wild-type *rx3* versus *rx3*^{ne2611} mRNA. Wild-type embryos were injected at the one-cell stage and observed at 24 hpf (lateral views, anterior left). Ectopic expression of *rx3* causes head truncations (L, arrow; compare with wild type, inset) whereas *rx3*^{ne2611} has no effect (M). (**N**) Percentage of embryos showing reduction of *tlc* expression (left two bars) (see Fig. S2 in the supplementary material) or head truncation (right two bars) following injection of *rx3* or *rx3*^{ne2611} mRNA (as indicated).

mutants at bud stage (Fig. 4H), but was expanded posteriorly from the one-somite stage onwards; *emx3* expression was unaffected in *ckh*^{ne2611} embryos until the 3-somite stage (Fig. 4K-M), only becoming visibly ectopic a few hours afterwards (not shown). Double stainings further demonstrated that *tlc* and *foxg1* expression largely overlaps *rx3* expression at the stages when they become ectopic in *ckh* (Fig. 4G,J), suggesting that these posterior expansions result from a failure to be repressed within the *rx3* domain. Accordingly, overexpression of *rx3*, but not *rx3*^{ne2611}, by mRNA injections into wild-type embryos, reduced expression of early telencephalic markers such as *tlc* and *hesx1* (*anf*) at the tail-bud stage (58% of cases, *n*=18; see Fig. S2 in the supplementary material; data not shown).

Given that *rx3* expression starts at late gastrulation, we conclude that telencephalic expansion in *ckh* reflects a role of Rx3 at its onset of expression in limiting telencephalic extent in the anterior neural plate. This function is normally manifested by the early downregulation of *tlc* expression within the *rx3*-positive domain, followed by the downregulation of *foxg1* and *emx3*.

Rx3 function accounts for the higher proliferation of eye-field cells when compared with telencephalic precursors

We next addressed the processes underlying this early function of Rx3. Several non-exclusive mechanisms affecting early telencephalic precursors might account for telencephalic expansion in *ckh*: their reduced cell death, their increased proliferation, or an ectopic specification of such precursors within the anterior neural plate. We analyzed cell death profiles in *ckh*^{ne2611} embryos between 90% epiboly and 3 somites using acridine orange and immunostaining of cleaved caspase 3. We did not detect any significant difference between mutant and wild-type siblings at these stages (n=19), although we did observe apoptosis in the telencephalon of *ckh*^{ne2611} mutants at 28 hpf (not shown).

We next monitored proliferation in the presumptive telencephalon and eye field using anti-phosphohistone H3 (PH3) immunocytochemistry. In wild-type embryos at tail-bud stage, the telencephalic anlage was identified by its expression of *tlc* (domain 3 in Fig. 5) and the eye field by *rx3* (domain 1 in Fig. 5). Corresponding domains in *ckh*^{ne2611} mutants were defined as *tlc* positive, *rx3* negative (domain 4 in Fig. 5), versus *rx3* positive (domain 2 in Fig. 5). Counts of PH3-positive cells within each domain revealed significantly decreased numbers of cells in M phase within the *rx3*-positive domain in *ckh*^{ne2611} when compared with wild-type siblings (P<0.02; compare domains 1 and 2), whereas proliferation within the more anterior *rx3*-negative domain is not affected (compare domains 3 and 4; P=0.86; Fig. 5A,B,E-G). This observation suggests either that Rx3 promotes proliferation inside the eye field during gastrulation, and/or that the acquisition of presumptive telencephalic identity imposes a low proliferation

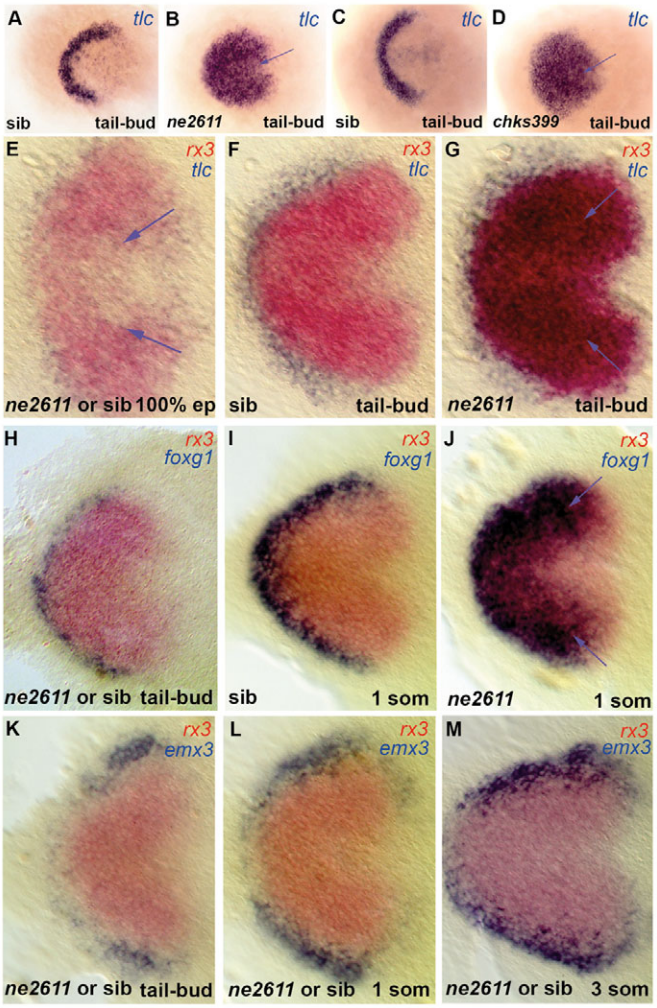

Fig. 4. Rx3 controls early patterning of the presumptive anterior forebrain. Expression of the markers indicated (color coded) in *ckh*^{ne2611} (B,G,J), *ckh*^{s399} (D) or their wild-type siblings (A,C,F,I); E,H,K-M are non-genotyped embryos from crosses between *ckh*^{ne2611}/+ heterozygotes. All views are dorsal anterior left in whole embryos (A-D) or flat mounts (E-M). (**A-D**) *tlc* expression identifies the presumptive telencephalon at tail-bud stage and is massively expanded in both *ckh*^{ne2611} (B) and *ckh*^{s399} (D) mutants compared with their wild-type siblings (A,C). (**E-G**) No difference in *tlc* expression is observed between wild-type and mutant embryos at 100% epiboly, when *tlc* expression is downregulated from the presumptive eye and hypothalamus fields, labeled by *rx3* (see the few remaining *tlc*-positive cells in the *rx3*-positive domain at 100% epiboly; arrows in E, absent in F). At tail-bud stage the ectopic *tlc* expression overlaps the *rx3* domain (G, blue arrows). (**H-J**) Expansion of *foxg1* across the eye field is absent at tail-bud stage (H) but is visible at the one-somite stage (J, blue arrows). (**K-M**) The relative expression of *emx3* and *rx3* are not noticeably affected in mutants before the 3-somite stage.

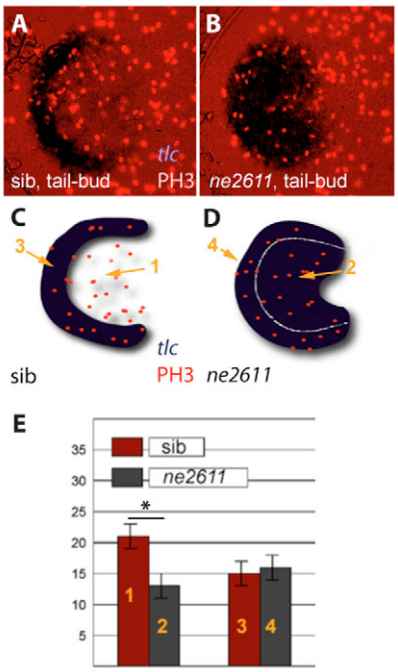

Fig. 5. Rx3 accounts for the higher proliferation of eye field versus telencephalic precursors. (**A**,**B**) Immunodetection of the M-phase marker Phosphohistone-H3 (red nuclei) in the anterior neural plate of *ckh*^{ne2611} mutants (right panel) and their wild-type siblings (left panel) at tail-bud stage (dorsal views, anterior left). *tlc* expression (ISH, blue) serves as a marker of the presumptive telencephalon in wild-type embryos and of the telencephalon+eye field in *ckh*^{ne2611}. (**C**,**D**) Schematic representation of the embryos in A,B to localize the presumptive telencephalic and eye fields in wild-type embryos (domains 3 and 1, respectively) and the corresponding territories in *ckh*^{ne2611} siblings (domains 4 and 2, respectively) at tail-bud stage. (**E**) Number of PH3-positive cells in domains 1-4 (see C,D) in wild-type (red) versus *ckh*^{ne2611} (gray) embryos. Bars indicate standard errors. Proliferation is significantly decreased in the presumptive eye field, but is unaltered in the presumptive telencephalon, in *ckh*^{ne2611} compared with wild-type embryos at tail-bud stage (two-sample independent Student's t-test, P values are given in the text).

rate. A role for Rx3 in controlling positively proliferation of retinal precursors had been suspected at the stage of optic vesicle evagination (Loosli et al., 2003). We show that Rx3 may exert this role already within the anterior neural plate.

Rx3 attributes eye versus telencephalic identity to anterior forebrain precursors

Decreased proliferation of retinal precursors might partially account for the lack of eyes of *ckh* mutants, but cannot be the direct cause of telencephalic expansion. By contrast, the co-expression of *tlc* or *foxg1* and mutant *rx3* RNAs in the presumptive eye-field territory of early *ckh*^{ne2611} embryos (Fig. 4G,J) suggests that telencephalic specification extends posteriorly at the expense of eye identity in the mutants.

To test this hypothesis, we traced the fate of eye-field precursors in *ckh*^{ne2611} mutants. Caged fluorescein was injected into one-cell stage embryos, and was activated in a small number (~10) of eye-field precursor cells at the early tail-bud stage (Fig. 6A,B); the location of the progeny of these labeled cells was then determined at 24 hpf by morphological inspection under fluorescence and Nomarski optics (Fig. 6C-I). At the early tail-bud stage, the eye and telencephalic fields are intermingled (Woo and Fraser, 1995); however, we found that uncaging at the position indicated in Fig. 6A mostly revealed retinal precursors in wild-type embryos (Table 1): pure retinal clones were recovered in 45% of cases (Fig. 6C), and clones contributing to the retina and other forebrain derivatives except the telencephalon in 45+21=66% of cases (Fig. 6D). This compared with 34% of cases contributing to the telencephalon (Fig. 6E; *n*=29). By contrast, all labeled clones contributed to the telencephalon in *ckh*^{ne2611} embryos (100% of cases, *n*=10; Table 1, Fig. 6F-I). Because extensive labeled clones were recovered in all activated *ckh*^{ne2611} mutants (Table 1), we conclude that retinal precursors lacking Rx3 tend to join the telencephalon. We never detected expression of retinal markers in the expanded telencephalon of *ckh*^{ne2611} (see *otx2* on Fig. 2B, or *atoh7* and *vax2*, not shown), supporting the interpretation that presumptive eye-field cells may acquire a telencephalic fate in the absence of Rx3 function.

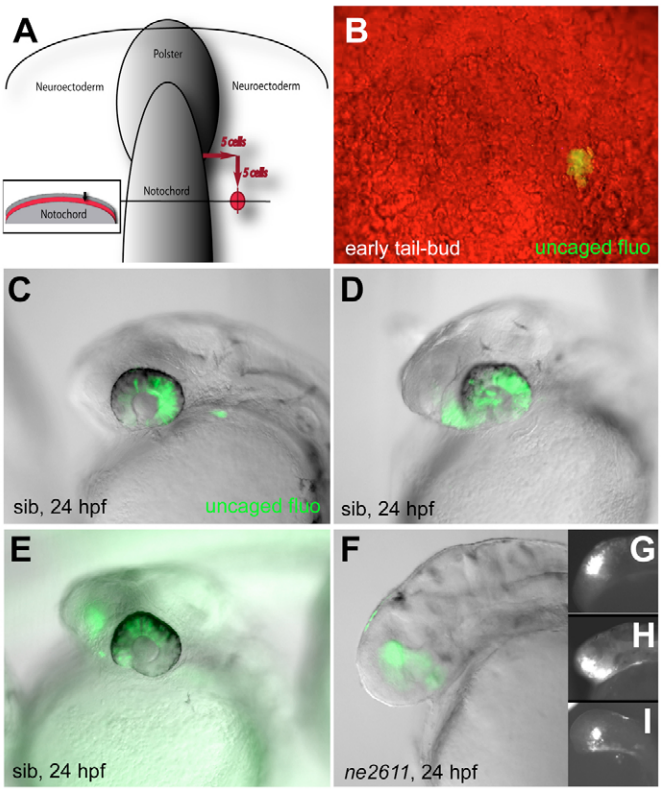

Fig. 6. Cells of the presumptive eye field acquire a telencephalic identity in the absence of Rx3. (**A**,**B**) Location of uncaged cells compared with the notochord, polster and enveloping layer (inset in A) at the early tail-bud stage, and photomicrograph of the fluorescent clone immediately following uncaging (B) (dorsal views, anterior up). (**C-E**) Fate of the uncaged progeny in wild-type embryos at 24 hpf (overlay of fluorescence and Nomarski optics views, anterior left). (C) Retina only (45% of cases); (D) retina and anterior hypothalamus (21% of cases); (E) retina and telencephalon (31% of cases) (see also Table 1). (**F-I**) Fate of the uncaged progeny in *ckh*^{ne2611} embryos at the 24 hpf stage (overlay of fluorescence and Nomarski optics views in F, fluorescence only in G-I, anterior left). All clones contribute to the telencephalon (100% of cases, see Table1).

The role of Rx3 in controlling retinal versus telencephalic identity is cell autonomous

Using transplantation experiments, Winkler et al. (Winkler et al., 2000) proposed that Medaka Eyeless, the ortholog of zebrafish Rx3, is responsible for retinal evagination in a cell-autonomous manner. The same is true for zebrafish Rx3: when large numbers of wild-type cells (25-40) are homotopically transplanted to the animal pole of a shield-stage *ckh*^{ne2611} embryo, they often give rise to a normally evaginated retina (36% of cases, *n*=11), which is always composed exclusively of wild-type cells (Fig. 7A). By contrast, *ckh*^{ne2611} cells transplanted into a wild-type host never contribute to the retina (not shown).

Our results support an earlier role of Rx3 in specification choices of eye field versus telencephalic identity. To determine whether this earlier function of Rx3 was also cell autonomous, we uncoupled it from morphogenesis control by transplanting a small number of cells (4-5). Indeed, we observed that when a low number of wild-type cells are transplanted into the presumptive eye field of a *ckh*^{ne2611} host, these integrate into the anterior forebrain and no evagination takes place (0% of cases, *n*=14; Fig. 7B). This finding suggests either that the wild-type cells are topologically misplaced in a mutant environment but keep their eye-field identity, or that when in a minority inside a Rx3-depleted environment, the wild-type cells are subjected to a non-autonomous cell fate change and adopt telencephalic identity.

To discriminate between these two possibilities and to assess the identity of the progeny of these transplanted cells, we made use of a sensitive transgenic retinal marker. In an enhancer detection screen following the technology described by Ellingsen et al. (Ellingsen et al., 2005), we recovered a transgenic line, *CLGY469*, which expresses YFP in the retina but not in the telencephalon (Fig. 7D). As mapping indicates, this line is likely to detect an *rx3* enhancer (see Materials and methods). YFP expression is observed in *CLGY469* transgenic embryos from the tail-bud stage onwards (see Fig. 7C for a 5-somite embryo), and thus precedes retinal evagination and is an early marker of retinal specification. We therefore used *CLGY469* expression as a selective and sensitive marker for retinal specification in our transplantation experiments with a low number of cells. When a few wild-type cells taken from the animal pole of a *CLGY469* transgenic donor were homotopically and isochronically transplanted into a *ckh*^{ne2611} non-transgenic host at the sphere stage, we repeatedly observed that some of these cells turn on expression of the transgene (80% of cases, *n*=5; Fig. 7F), in

Table 1. Fate of cell clones uncaged, as indicated in Fig. 6A, at the early tail-bud stage in wild-type and *ckh*^{ne2611} mutant siblings

	Wild type					*chokh*^{ne2611}		
		Ret w/o Tel		Tel±others			Tel±others	
Experiment	*n*	Retina only	Ret+ventral CNS*	Ret+Tel	Tel	*n*	Tel	Tel+Tec
1	3	1	1	1	0	1	1	0
2	12	4	3	4	1	2	2	0
3	5	3	2	0	0	3	2	1
4	7	4	0	3	0	2	2	0
5	2	1	0	1	0	2	2	0
Sum	29	13	6	9	1	10	9	1
%	100	45	21	31	3	100	90	10
Total %		66		34			100	

*Ventral structures of the rostral CNS (optic nerve and hypothalamus).
Five independent experiments were conducted. Labeled clones were recovered in all embryos. The values listed are the number (or percentage) of uncaged embryos where labeled clones contribute to the structures indicated.
Ret, retina; Hyp, hypothalamus; Tel, telencephalon; Tec, tectum.

conditions where no morphological retina is visible. We can rule out that the transplanted cells, although YFP-negative at the time of transplantation, were already determined to express the transgene: similar grafts into non-transgenic wild-type hosts usually gave rise to YFP expression in cells that populated the retina, but not in cells that contributed to other structures (usually the telencephalon; Fig. 7G; 86% of cases, *n*=7). We conclude that the maintenance of eye-field identity, and repression of telencephalon fate, is cell-autonomously encoded by Rx3 expression.

DISCUSSION

Our results demonstrate that, at late gastrulation, zebrafish Rx3 is the determinant biasing cells of the eye field towards a retinal fate at the expense of a telencephalic fate. This function is performed in a cell-autonomous manner, and is accompanied by the repression of *tlc* and *foxg1* expression by Rx3. These findings, which identify a molecular component of the anterior forebrain-patterning cascade, shed light on the processes segregating the telencephalon and eye field during anterior forebrain patterning. Given the previously demonstrated roles of Rx3 in controlling retinal evagination (Kennedy et al., 2004; Loosli et al., 2003; Loosli et al., 2001; Winkler et al., 2000) and formation of the pigmented retinal epithelium (Rojas-Munoz et al., 2005), they also suggest that the link between several crucial steps of retinal development, namely the maintenance of retinal precursors, the morphogenetic shaping of the retina into an optic cup and the specification of the pigmented retinal epithelium, are accomplished at least in part by the use of the same molecule, Rx3.

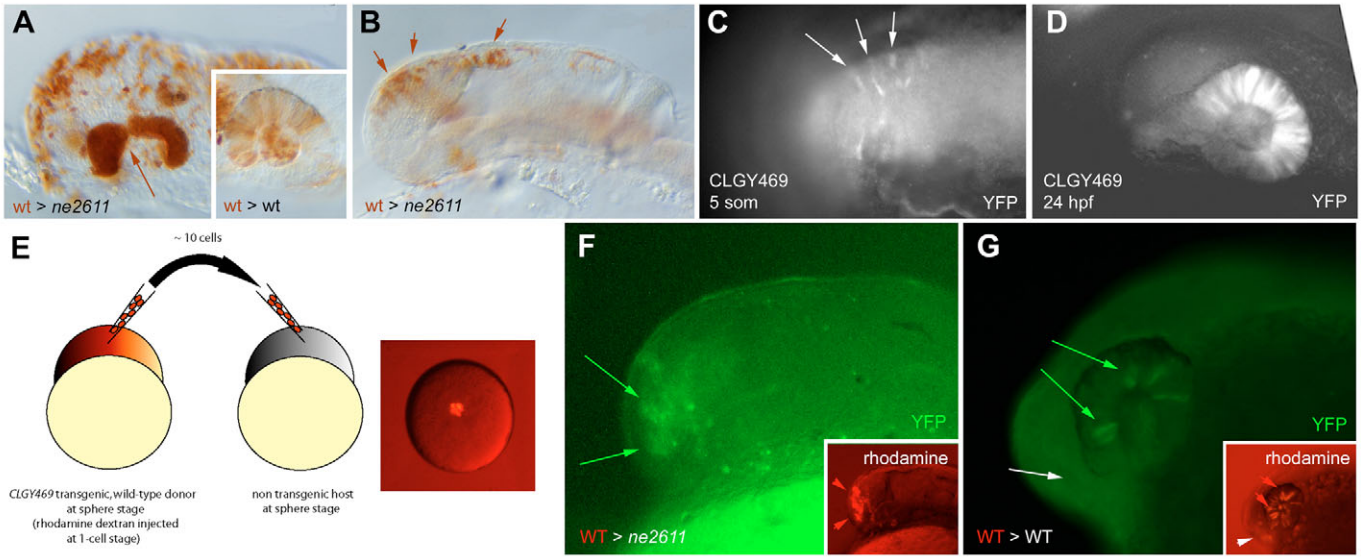

Fig. 7. Rx3 controls eye field versus telencephalic fate in a cell-autonomous manner. (**A,B**) Transplantation of wild-type cells (brown) into the anterior forebrain of a *ckh*^{ne2611} or wild-type (inset) host. (A) When a large number of cells are transplanted, retinal structures are rescued and evaginate (arrow). They are entirely composed of wild-type cells, whereas transplanted cells distribute randomly in a wild-type host (inset). (B) When a low number of cells is transplanted, retinal evagination does not occur. (**C,D**) Expression of YFP (revealed by anti-GFP immunocytochemistry) in transgenic *CLGY469* embryos before (C; dorsal view) and after (D; lateral view) retinal evagination. YFP expression is restricted to eye-field cells and their descendants. It is absent in *ckh*^{ne2611} mutants (see text). (**E-G**) Transplantation of a few wild-type cells transgenic for *CLGY469* into the animal pole of a *ckh*^{ne2611} (F) or wild-type (G) host. In a mutant host (F), retinal evagination does not occur (as in B), but expression of the transgene (green) is rescued in some transplanted cells (red, inset), indicating rescue of the eye-field fate. In a wild-type host, transplanted cells contribute to the retina (red arrowheads) and telencephalon (white arrowhead; G, inset), but only retinal cells express the transgene (G, green arrows, as opposed to white arrow).

The complete *ne2611* phenotype results from the loss of Rx3 function

Previous analyses of *ckh* mutant alleles did not report telencephalic defects (Kennedy et al., 2004; Loosli et al., 2003; Rojas-Munoz et al., 2005), making it crucial to ascertain that the *ne2611* phenotype results solely from the loss of Rx3 function. Our observations that telencephalic and eye phenotypes in *ckh*^{ne2611} always co-segregate and are concomitantly rescued by injection of an *rx3*-containing BAC support the interpretation that Rx3, directly or indirectly, controls the early development of both telencephalon and eyes. A further decisive argument towards this interpretation is provided by our re-analysis of *ckh*^{s399}, and the finding that *ckh*^{s399} mutants display expanded *tlc* and *emx3* expression from the tail-bud and somite stages onwards, respectively, in a manner indistinguishable from *ckh*^{ne2611} (Fig. 3F, Fig. 4D). These observations lead us to propose an early role for Rx3 in limiting extension of the telencephalic field at late gastrulation. This finding is in keeping with the onset of zebrafish *rx3* expression during gastrulation, earlier than *rx1* and *rx2*, and in a domain adjacent to but non-overlapping with the presumptive telencephalon (Chuang et al., 1999). The phenotype of *Rx* mutant mice is complex and includes both lack of eyes and anterior forebrain truncations (Mathers et al., 1997). Given that the mouse harbors a single *Rx* gene, successive functions for Rx might be difficult to appreciate experimentally; however, the precocious downregulation of retinal markers in these mutants is compatible with an early role of Rx in controlling retinal specification. Medaka, where loss of Rx3/el seems to be only associated with morphogenesis defects, is a more puzzling case (Loosli et al., 2001; Winkler et al., 2000). Unlike zebrafish Rx3 (Chuang and Raymond, 2001) (this paper), overexpression of Rx3/el in Medaka does not cause head truncations (Loosli et al., 2001). Rx3/el can, however, rescue the *ckh* phenotype (Loosli et al., 2003). Thus, zebrafish Rx3 and Medaka Rx3/el might have similar regulatory capacities, but not all can be revealed in the Medaka context. This observation might relate to the recent demonstration of a genetic background-dependent effect of Rx3 in zebrafish (Rojas-Munoz et al., 2005). However, the evolutionary conservation of an early expression of Rx genes during brain development in vertebrates and invertebrates (Bailey et al., 2004) lends support to a primary ancestral role of Rx in the specification of early anterior progenitors.

Rx3 function maintains retinal versus telencephalic identity

The expanded telencephalon and lack of eyes of *ckh* mutants might have been subsequent but unrelated phenomena reflecting two independent roles of Rx3. Contrary to this hypothesis, we found that retinal precursors, although at least partially specified (e.g. expressing *rx3* and *rx1* RNAs, Fig. 2C-D,H), are affected already at late gastrulation in *ckh*^{ne2611} mutants. This is noticeable in two ways: first, their proliferation is reduced (Fig. 5B,E); and second, their identity is altered, as revealed by the co-expression of *tlc* or *foxg1* and *rx3* within the eye field in *ckh*^{ne2611} at the tail-bud or one-somite stage (Fig. 4G,J), combinations never observed in wild-type embryos. Direct tracing of eye-field cells from the tail-bud stage further demonstrates that these cells, in mutants, populate the telencephalon instead of the retina and probably acquire a telencephalic fate (Fig. 6). Together, these results are best interpreted by postulating an early role of Rx3 in permitting the maintenance of retinal versus telencephalic specification during gastrulation.

Based on overexpression studies, zebrafish Rx1 and Rx2 were postulated to promote retinal versus telencephalic identity (Chuang and Raymond, 2001). Notably however, the telencephalic to retinal fate switch imposed by injection of *rx1* or *rx2* mRNA was only observed at a late stage (neural keel), while no alteration in *emx3* or *foxg1* expression could be detected at the neural plate stage. It will be important to support these data by loss-of-function analyses to determine whether the distinction between the eye and telencephalic identities is a general property of Rx factors, and, if so, whether these factors act in a timely regulated cascade.

An additional phenotype of *ckh*^{ne2611} mutants is the decreased proliferation of eye-field precursors at the tail-bud stage (Fig. 5), suggesting that Rx3, in addition to imparting cell identity, also promotes proliferation of its expressing cells at late gastrulation. This finding is in line with previous analyses of *Xenopus* Xrx1, which has been shown to increase the clonal proliferation of retinal progenitors in ectopic expression experiments (Casarosa et al., 2003). Whether the impaired proliferation of the eye field in *ckh*^{ne2611} mutants is a consequence of the altered identity of these cells or reflects an independent role of Rx3 in proliferation control remains to be resolved. Similarly, Xrx1 promotes both proliferation and retinal identity.

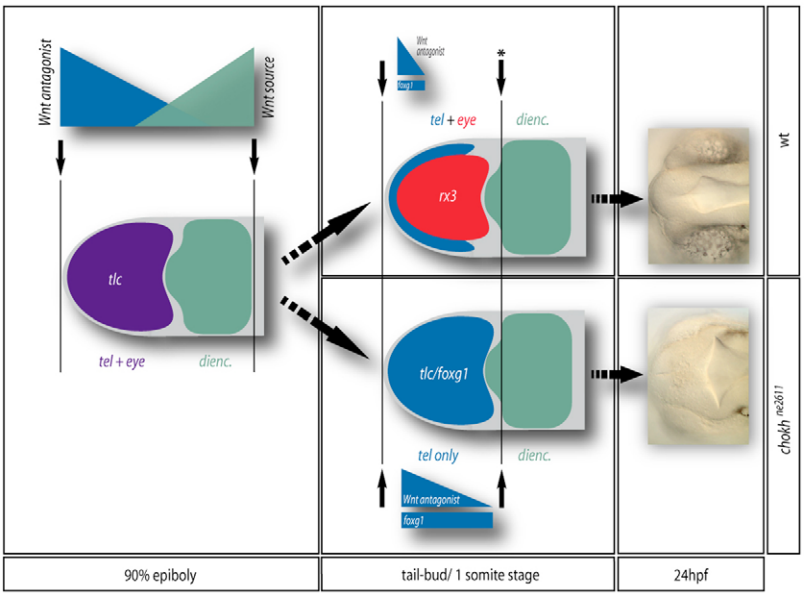

Fig. 8. Model for the segregation of the telencephalic and eye anlage during zebrafish forebrain patterning. Patterning boundaries are indicated by black arrows. During gastrulation (left panel), a prevalent view is that the forebrain is patterned as a whole by the opposite activities of a posterior Wnt source located at the level of the posterior diencephalon (green gradient) and Wnt antagonists (purple gradient) located at the ANB (Wilson and Houart, 2004). 'High Wnt' defines the presumptive diencephalon (green), whereas 'low Wnt' defines an anterior domain (purple) including the presumptive telencephalon and eyes. At the tail-bud stage (middle panel), a posterior patterning boundary (black arrow with star) is set-up in front of the diencephalon, isolating the anterior forebrain. Within the latter domain, Rx3 activity (red) represses *tlc* expression (blue gradient) and *foxg1* (blue bar) and attributes retinal fate to its expressing cells at the expense of a telencephalic fate, thereby segregating retinal and telencephalic identities (top panel). In the absence of Rx3, retinal precursors acquire a telencephalic fate (bottom panel), leading at 24 hpf to the absence of eyes and an enlarged telencephalon (right panel).

Molecular cascade of Rx3 function in the development of the presumptive eye field versus telencephalon

The initiation of *rx3* expression does not depend on Pax6 or Six3 (Carl et al., 2002), and identifying the upstream regulators of the Rx3-mediated retinal specification cascade will be an important step in our understanding of anterior forebrain patterning. Known targets of Rx3 include *rx2* and *mab21l2*, which are absent or downregulated in *ckh* (Kennedy et al., 2004). *six3* or *pax6.1* expression appeared unaffected in *ckh*^{ne2611} at the 3-somite stage (not shown); however, both genes also label the telencephalic primordium at that stage, preventing a straightforward interpretation of these results. We identify here, however, two new and possibly important targets of Rx3: *tlc* and *foxg1*. Their expression is modified in *ckh*^{ne2611} prior to the normal timing of optic vesicle evagination, strongly suggesting that these genes respond to the early function of Rx3. Whether Rx factors display transcriptional repressor or activator functions is unresolved (Chuang and Raymond, 2001), and our results do not permit us to determine whether the regulation of expression of *tlc* and *foxg1* by Rx3 is direct.

Finally, we observed that *ckh*^{ne2611} cells transplanted into the animal pole of a wild-type host preferentially populate the telencephalon (not shown). Thus, in addition to attributing an eye-field identity to its expressing cells, Rx3 may also endow these cells with specific cell surface recognition properties that distinguish them from telencephalic precursors. This phenomenon might be an integral part of the Rx3-encoded specification maintenance process.

A model for the subdivision of the anterior forebrain into telencephalon and eye field

A major finding of our study is that, at late gastrulation, Rx3 controls cell identity choices between the presumptive telencephalic and retinal fields but spares most other diencephalic domains, with the possible exception of the anterior hypothalamus (see Fig. 1E-I). These results permit for the first time the proposal of a model for the segregation of the telencephalon and eye field (Fig. 8). Following global AP forebrain patterning during gastrulation, a boundary of the patterning field is established between the diencephalon and eye field (Fig. 8, asterisk), demarcating the posterior limit of a patterning process specific to the anterior forebrain and segregating eye versus telencephalic identities. Without Rx3 function, retinal precursors adopt a telencephalic fate, demonstrating that Rx3 biases cell fate choices in bipotential precursors. Whether telencephalic precursors at that stage would also be capable of acquiring a retinal fate remains to be demonstrated. It is also unknown whether these precursors are defined by default by the absence of Rx3 expression, or whether they also necessitate instructive information.

Whether the specific Rx3-mediated anterior forebrain patterning process involves graded positional information, in a manner reminiscent of global forebrain patterning at an earlier stage (Wilson and Houart, 2004), remains unknown. Several findings suggest a possible involvement of Wnt signaling in this early Rx3-dependent process. First, the earliest alteration in gene expression in *ckh*^{ne2611} is the ectopic maintenance of *tlc* expression (Fig. 4A-G; Fig. 8, blue gradient). Second, overexpression of *rx3* by mRNA injection leads to head truncations (Fig. 3), and a similar phenotype is caused by exaggerated Wnt signaling (Kim et al., 2000). Thus, the Rx3 overexpression phenotype might result from a (premature) positive interaction of Rx3 with Wnt activity. Finally, olSfrp1, which was recently proposed to also participate in anterior forebrain patterning, belongs, like Tlc, to the sFRP family of Wnt-binding factors (Esteve et al., 2004). Thus, whether Tlc activity is instrumental in the anterior forebrain cell-specification defects of *ckh*^{ne2611}, and whether an appropriate source of Wnt is positioned at the eye field/diencephalon border at late gastrulation, remain important issues to address. Another, non-exclusive, interesting candidate that might account for the *ckh*^{ne2611} phenotype is Foxg1 (Fig. 8, blue bars). However, the early expression domain of *foxg1*, in wild type, is not completely restricted to the telencephalic primordium but also includes a small portion of the ventral retinal field (Lisa Winstanley and C.H., unpublished). Thus, Foxg1 involvement in telencephalic versus eye specification would be complex and is likely to imply context-dependent activities, which might be related to the presence or absence of Rx3.

We are grateful to K. Imai, R. Koester and other lab members for critical advice during this work, to H. Baier and J. Wittbrodt for the *ckh*^{s399} line, to F. Rosa for help with ENU mutagenesis, and to numerous colleagues for the gift of probes. C.S. and L.B.-C. are supported by a VW Stiftung junior group grant, and C.S., L.B.-C. and T.S.B. by EU 6th Framework contract number LSHC-CT-2003-503466. Work in T.S.B.'s laboratory is further supported by a Sars Centre core grant, by the National Programme in Functional Genomics in Norway (FUGE) in the Research Council of Norway, and by additional funding from the University of Bergen.

Supplementary material

Supplementary material for this article is available at
http://dev.biologists.org/cgi/content/full/133/15/2925/DC1

References

Bailey, T. J., El-Hodiri, H., Zhang, L., Shah, R., Mathers, E. H. and Jamrich, M. (2004). Regulation of vertebrate eye development by Rx genes. *Int. J. Dev. Biol.* **48**, 761-770.

Carl, M., Loosli, F. and Wittbrodt, J. (2002). Six3 inactivation reveals its essential role for the formation and patterning of the vertebrate eye. *Development* **129**, 4057-4063.

Casarosa, S., Amato, M. A., Andreazzoli, M., Gestri, G., Barsacchi, G. and Cremisi, F. (2003). Xrx1 controls proliferation and multipotency of retinal progenitors. *Mol. Cell. Neurosci.* **22**, 25-36.

Chuang, J. C. and Raymond, P. A. (2001). Zebrafish genes rx1 and rx2 help define the region of forebrain that gives rise to retina. *Dev. Biol.* **231**, 13-30.

Chuang, J., Mathers, P. and Raymond, P. (1999). Expression of three Rx homeobox genes in embryonic and adult zebrafish. *Mech. Dev.* **84**, 195-198.

Cuff, J. A., Clamp, M. E., Siddiqui, A. S., Finlay, M. and Barton, G. J. (1998). JPred: a consensus secondary structure prediction server. *Bioinformatics* **14**, 892-893.

Dorsky, R. I., Itoh, M., Moon, R. T. and Chitnis, A. (2003). Two tcf3 genes cooperate to pattern the zebrafish brain. *Development* **130**, 1937-1947.

Eagleson, G. W. and Dempewolf, R. D. (2002). The role of the anterior neural ridge and Fgf-8 in early forebrain patterning and regionalization in Xenopus laevis. *Comp. Biochem. Physiol. B Biochem. Mol. Biol.* **132**, 179-189.

Ellingsen, S., Laplante, M. A., König, M., Kikuta, H., Furmanek, T., Hoivik, E. A. and Becker, T. S. (2005). Large-scale enhancer detection in the zebrafish genome. *Development* **132**, 3799-3811.

Esteve, P., Lopez-Rios, J. and Bovolenta, P. (2004). SFRP1 is required for the proper establishment of the eye field in the medaka fish. *Mech. Dev.* **121**, 687-701.

Foley, A. C. and Stern, C. D. (2001). Evolution of vertebrate forebrain development: how many different mechanisms? *J. Anat.* **199**, 35-52.

Graw, J. (2003). The genetic and molecular basis of congenital eye defects. *Nat. Rev. Genet.* **4**, 876-888.

Haffter, P., Granato, M., Brand, M., Mullins, M. C., Hammerschmidt, M., Kane, D. A., Odenthal, J., van Eeden, F. J., Jiang, Y. J., Heisenberg, C. P. et al. (1996). The identification of genes with unique and essential functions in the development of the zebrafish, Danio rerio. *Development* **123**, 1-36.

Hammerschmidt, M., Pelegri, F., Mullins, M. C., Kane, D. A., van Eeden, F. J., Granato, M., Brand, M., Furutani-Seiki, M., Haffter, P., Heisenberg, C. P. et al. (1996). dino and mercedes, two genes regulating dorsal development in the zebrafish embryo. *Development* **123**, 95-102.

Hanson, I. M. (2003). PAX6 and congenital eye malformations. *Pediatr. Res.* **54**, 791-796.

Heisenberg, C. P., Houart, C., Take-Uchi, M., Rauch, G. J., Young, N., Coutinho, P., Masai, I., Caneparo, L., Concha, M. L., Geisler, R. et al. (2001). A mutation in the Gsk3-binding domain of zebrafish Masterblind/Axin1 leads to a fate transformation of telencephalon and eyes to diencephalon. *Genes Dev.* **15**, 1427-1434.

Ho, R. K. and Kane, D. A. (1990). Cell-autonomous action of zebrafish spt-1 mutation in specific mesodermal precursors. *Nature* **348**, 728-730.
Houart, C., Westerfield, M. and Wilson, S. W. (1998). A small population of anterior cells patterns the forebrain during zebrafish gastrulation. *Nature* **391**, 788-792.
Houart, C., Caneparo, L., Heisenberg, C., Barth, K., Take-Uchi, M. and Wilson, S. (2002). Establishment of the telencephalon during gastrulation by local antagonism of Wnt signaling. *Neuron* **35**, 255-265.
Kelly, G. M., Greenstein, P., Erezyilmaz, D. F. and Moon, R. T. (1995). Zebrafish wnt8 and wnt8b share a common activity but are involved in distinct developmental pathways. *Development* **121**, 1787-1799.
Kennedy, B. N., Stearns, G. W., Smyth, V. A., Ramamurthy, V., Van Eeden, F., Ankoudinova, I., Raible, D., Hurley, J. B. and Brockerhoff, S. E. (2004). Zebrafish rx3 and mab21l2 are required during eye morphogenesis. *Dev. Biol.* **270**, 336-349.
Kim, C. H., Oda, T., Itoh, M., Jiang, D., Artinger, K. B., Chandrasekharappa, S. C., Driever, W. and Chitnis, A. B. (2000). Repressor activity of Headless/Tcf3 is essential for vertebrate head formation. *Nature* **407**, 913-916.
Kimmel, C. B., Ballard, W. W., Kimmel, S. R., Ullmann, B. and Schilling, T. F. (1995). Stages of embryonic development of the zebrafish. *Dev. Dyn.* **203**, 253-310.
Lagutin, O. V., Zhu, C. C., Kobayashi, D., Topczewski, J., Shimamura, K., Puelles, L., Russell, H. R., McKinnon, P. J., Solnica-Krezel, L. and Oliver, G. (2003). Six3 repression of Wnt signaling in the anterior neuroectoderm is essential for vertebrate forebrain development. *Genes Dev.* **17**, 368-379.
Loosli, F., Winkler, S., Burgtorf, C., Wurmbach, E., Ansorge, W., Henrich, T., Grabher, C., Arendt, D., Carl, M., Krone, A. et al. (2001). Medaka eyeless is the key factor linking retinal determination and eye growth. *Development* **128**, 4035-4044.
Loosli, F., Staub, W., Finger-Baier, K. C., Ober, E. A., Verkade, H., Wittbrodt, J. and Baier, H. (2003). Loss of eyes in zebrafish caused by mutation of chokh/rx3. *EMBO Rep.* **4**, 894-899.
Mathers, P. H. and Jamrich, M. (2000). Regulation of eye formation by the Rx and pax6 homeobox genes. *Cell. Mol. Life Sci.* **57**, 186-194.
Mathers, P. H., Grinberg, A., Mahon, K. A. and Jamrich, M. (1997). The Rx homeobox gene is essential for vertebrate eye development. *Nature* **387**, 603-607.
Rojas-Munoz, A., Dahm, R. and Nusslein-Volhard, C. (2005). chokh/rx3 specifies the retinal pigment epithelium fate independently of eye morphogenesis. *Dev. Biol.* **288**, 348-362.
Shimamura, K. and Rubenstein, J. L. (1997). Inductive interactions direct early regionalization of the mouse forebrain. *Development* **124**, 2709-2718.
van de Water, S., van de Wetering, M., Joore, J., Esseling, J., Bink, R., Clevers, H. and Zivkovic, D. (2001). Ectopic Wnt signal determines the eyeless phenotype of zebrafish masterblind mutant. *Development* **128**, 3877-3888.
Wilson, S. W. and Houart, C. (2004). Early steps in the development of the forebrain. *Dev Cell* **6**, 167-181.
Winkler, S., Loosli, F., Henrich, T., Wakamatsu, Y. and Wittbrodt, J. (2000). The conditional medaka mutation eyeless uncouples patterning and morphogenesis of the eye. *Development* **127**, 1911-1919.
Woo, K. and Fraser, S. E. (1995). Order and coherence in the fate map of the zebrafish nervous system. *Development* **121**, 2595-2609.